JST

JOURNAL OF SCIENCE AND TECHNOLOGY
ISSN: 2229-8460 e-ISSN: 2600-7924

Vol. 18 No. 1 (2026) 142-154
https://publisher.uthm.edu.my/ojs/index.php/jst

Performance of Green Zinc Oxide Nanofluids in Membrane Photocatalytic Reactor: The Effect of Nanofluids Concentration

Muhammad Akmal Hisyam Idris[1], Muhammad Akmal Annuar[1], Muhammad Zharif Mohd Zamirullah[1], Noor Atiqah Zuraini[2], Dilaeleyana Abu Bakar Sidik[1]*, Nur Hanis Hayati Hairom[2], Zarizi Awang[2], Maskhairiah Ismail[3], Noor Yahida Yahya[4,5]

[1] *Centre for Diploma Studies, Universiti Tun Hussein Onn Malaysia, Muar, Johor, 84600, MALAYSIA*
[2] *Faculty of Engineering Technology, Universiti Tun Hussein Onn Malaysia, Muar, Johor, 86400, MALAYSIA*
[3] *Samsung SDI Energy Malaysia Sdn Bhd., Sungai Gadut Negeri Sembilan, 71450 MALAYSIA*
[4] *Faculty of Civil Engineering Technology, Universiti Malaysia Pahang Al–Sultan Abdullah, Kuatan, Pahang, 26300, MALAYSIA*
[5] *Centre for Advanced Intelligent Materials, Universiti Malaysia Pahang Al–Sultan Abdullah, Kuatan, Pahang, 26300, MALAYSIA*

*Corresponding Author: dila@uthm.edu.my
DOI: https://doi.org/10.30880/jst.2026.18.01.013

Article Info

Received: 3 January 2026
Accepted: 2 May 2026
Available online: 27 June 2026

Keywords

Zinc oxide, nanofluids, palm oil mill secondary effluent, membrane photocatalytic reactor

Abstract

Recently, researchers exploring membrane photocatalytic reactor (MPR) treatment employing Zinc Oxide (ZnO) nanoPARticles incorporated capping agents due to their ability to boost photocatalytic performance and reduce fouling. The performance of ZnO–incorporated Pandanus amaryllifolius Roxb. nanofluids (ZnO–PAR) at varying concentrations for palm oil mill secondary effluent (POMSE) treatment via MPR was the main focus of this investigation. The maximum removal effectiveness of color (99.2%), total suspended solid (TSS) (93.6%), turbidity (95.6%), chemical oxygen demand (COD) (96.8%), permeate flux (23.9±0.3 L/m^2.hr) and normalized flux (0.47) was achieved at 1.0 wt% ZnO–PAR nanofluids. According to this study, 1.0 wt% produced an ideal balanced and effective performance, demonstrating the substantial potential for use in the palm oil sector since it optimized flux and minimize membrane fouling. While the highest pollutant removal efficiencies were achieved at the lower concentrations (0.1 and 0.25 wt%). This green nanotechnology provides a viable tertiary treatment solution that meets environmental discharge limits outlined in Malaysia's Environmental Quality Act 1974.

1. Introduction

Palm oil mill effluent (POME) is a brown viscous liquid waste with a strong odor and a high concentration of colloidal suspensions, as well as a large amount of biological material. The anaerobic treatment of POME is also referred to as palm oil mill secondary effluent (POMSE) because it has undergone secondary treatment. Although the POMSE has undergone several series of treatments, the characteristics of the POMSE still do not meet the discharged criterion by the Department of Environment, where the values of the chemical oxygen demand (COD: 150–2800 mg/L) and (BOD: 250–580 mg/L) remain high and are considered dangerous for discharge [1]. Furthermore, the values of discharge standard set by Department of Environment (DOE), where the values of the chemical oxygen demand (COD: <100 mg/L) and biochemical oxygen demand (BOD: >20 mg/L) to protect water quality by preventing excessive organic pollution and ensuring ecosystem safety [2]. For treating POMSE besides using method membrane photocatalytic reactor (MPR), there are various methods like photocatalysis, membranes, Fenton and electrolysis treatment. Each system of them has disadvantages, like photocatalytic treatment requires UV–light, which is high cost for the maintenance, catalyst like TiO_2 can deactivate due to organic fouling and for COD and BOD removal only ~60–80% (insufficient for DOE Standard B) [1]. Furthermore, for membrane filtration, the disadvantages are the membrane often fouling, which is reduced flux over time, high maintenance (frequent cleaning needed) and often requires pretreatment to ensure optimum performance of reverse osmosis (RO) systems [2]. Other than that, for treatment method Fenton produces toxic iron sludge that requires disposal and requires very low pH (pH 2–3). Thus, for COD removal almost ~70–90%, but BOD remains high [3]. Lastly, for electrolysis (electrochemical treatment), there are expensive electrodes like platinum (Pt), and boron–doped diamond, high energy consumption and inconsistent removal (~50–80%) [4].

MPR is one promising approach for treating secondary effluent POMSE. The MPR technique utilizes a type of reactor that integrates membrane technology with photocatalysis. It employs a membrane that serves two functions: as a selective filter that allows certain molecules through while blocking others, and as a physical barrier that prevents the photocatalyst from entering the reaction mixture. The photocatalyst may be immobilized on the surface of the membrane (photocatalytic membranes) or suspended in the reaction mixture. MPR has several advantages over conventional approaches, including increased photocatalyst capacity, simultaneous photocatalyst and membrane filtration, precise control over residence duration, and confinement of the photocatalyst within the membrane's environment [5]. Previous research by Awang et al. [6] and Sidik et al. [7] reveals that MPR performs excellently in treating POMSE in terms of color removal (>90%). However, membrane fouling is seen as a key obstacle in MPR systems incorporating nanoparticles. This problem is believed to be remedied by selecting the best photocatalyst in the MPR system.

Photocatalysis is an approach of stimulating chemical processes using light energy. Photocatalysis has sparked widespread interest as a promising strategy for decreasing pollution in the environment [2]. Additionally, it is a light–induced catalytic mechanism that, when exposed to light above the bandgap, causes redox reactions that reduce or oxidize organic molecules by generating electron–hole pairs on the surface of metal oxide semiconductors [8]. Recently, photocatalytic technology in the palm oil mill industry has emerged as another intriguing treatment avenue for wastewater pollution management and reduction [9]. The effectiveness of the photocatalytic degradation process can be influenced by the photocatalyst used. The effectiveness of the degradation process can be enhanced by changing the photocatalyst, this increases the surface area that may be used for the reaction's UV light adsorption [10].

There are numerous techniques for altering the size, shape, and morphology of metal nanoparticles (NPs) generated from plant extracts. The production of NPs from greener raw materials has sparked a lot of attention due to its medicinal potential and environmental benefits over traditional chemical techniques. Our previous study using Cymbopogon citratus leaf extract and ZnO demonstrated improved degradation efficiency on high strength wastewater in a photocatalytic membrane reactor system. Because of the large size and durability of ZnO NPs, biosynthesis of NPs from plants is the best way to improve performance in photocatalytic systems [7].

Nanofluids have sparked a lot of interest due to their excellent physicochemical and thermal properties. These are nanoparticle colloidal suspensions created using a base fluid. Nanofluids are potential prospects for a variety of applications in industries ranging from wastewater treatment to electronics cooling due to their improved properties, which include increased thermal conductivity, higher heat transfer rates, and fewer fouling tendencies [11]. To lessen their environmental impact, recent developments have focused on creating economically and environmentally friendly processes for creating nanofluids using green chemistry approaches. The tendency of ZnO nanofluids to agglomerate and aggregate throughout the synthesis process can be reduced using a biological capping agent. Modified ZnO nanofluids are thought to have the ability to address photocatalytic and membrane fouling issues in the MPR system.

Yahya et al. [12] proposed an ecological technique to produce biosorbent utilizing Pandanus amaryllifolius Roxb (PAR) leaves to remove Chromium (VI) ions in wastewater. In addition, previous study by Haththotuwa and Amarasinghe [13] shows PAR adsorbent can remove selected textile dyes up to 95%. Wang et al. [14] reported that PAR extract has a high total phytoconstituent such as terpenoids, alkaloid, phenolic and flavanoids. These

J. of Science and Technology Vol. 18 No. 1 (2026) p. 142-154

phenolic substances can function as reducing, stabilizing, and agglomeration–preventative agents, which may be employed in the synthesis of nanoparticles [15]. This discovery confirmed that PAR has a great potential as a capping agent by modifying with the ZnO nanoparticles. A higher efficiency of the degradation process and a lower fouling tendency can be accomplished by modifying the photocatalyst, which provides a larger surface area for UV–light adsorption during the reaction.

Unfortunately, there is still a dearth of knowledge about the development of a simpler technique for the environmentally friendly synthesis of ZnO nanofluids (NFs) employing PAR as a capping agent. Furthermore, there has never been an attempt to synthesize ZnO NFs sustainably using PAR for the treatment of POMSE in the MPR system. Therefore, the purpose of this project is to investigate the effect of various concentration for ZnO–PAR NFs in a MPR for POMSE treatment.

2. Materials

The aged PAR leaves which have darker color (age > 1 month) were used due to the higher phenolic compound [16]. The PAR leaves were gathered from a rural area in the Pagoh, Johor, Malaysia. The POMSE samples were collected from the aerobic pond of an adjacent oil palm company in Pagoh, Johor, Malaysia. To avoid contamination during processing the samples, the POMSE samples were kept at 4°C and in the dark. Identical batches of POMSE were used in each experimental trial to guarantee the homogeneity of POMSE composition. BT Science Sdn Bhd, Malaysia, provided the chemicals, which included zinc acetate (Bendosen), oxalic acid (Sisco Research Laboratories, SRL), choline chloride (Chemiz) and urea (Chemiz).

2.1 Synthesis ZnO–PAR Nanofluids

Fresh leaves were used as reducing and capping agents in the synthesis of tiny metal nanoparticles. PAR leaves were first washed with tap water to remove any foreign particles, insects, or dust. The leaves were sun–dried for a whole day. After that, the leaves were ground in a blender and sieved until they reached a fine powder with a size of 100 microns. According to Sidik et al. [7], the powdered PAR leaves were combined with de–ionized water at a ratio of 1:30 and then incubated for 60 minutes at 80°C and 180 rpm in an incubator shaker. The extracted liquid was then filtered via Whatman No.1 filter paper. The PAR leaf extract was transferred to a sealed container and stored in a freezer at 4°C to ensure purity and availability for use.

Precipitation techniques were used to synthesize ZnO–PAR nanoparticles, according to Sidik et al. [7] Zinc acetate dehydrate (0.1 M) was mixed with 0.15 M oxalic acid dehydrate at ambient temperature (25°C). After 5 minutes, the reaction mixture containing ZnO was added to the PAR leaf extract in a 3:1 ratio. The solution was shaken in an incubator shaker under 180 rpm for 24 hours at 25°C in order to further boost the synthesis of ZnO. The precipitate was filtered by suction through Whatman No. 1 filter paper, and the water was subsequently eliminated by heating it for 1 hour at 100°C in an oven [7,17,18]. The precipitate was calcined in a furnace (Model: Nabertherm) for 2 hours at 550◦C to eliminate any remaining impurities. The calcination produced a white powder containing ZnO–PAR nanoparticles. X-ray diffraction (XRD Model; Brukar D8) was used to analyze the ZnO-PAR nanoparticles and validate their purity. The XRD patterns of green-synthesized ZnO–PAR nanoparticles are shown in Fig. 1 exhibited well-defined diffraction peaks at $2\theta \approx 31.7°$, 34.4°, 36.2°, 47.5°, 56.6°, 62.9°, 66.3°, 67.9°, and 69.1° which are indexed to the (100), (002), (101), (102), (110), (103), (200), (112) and (201) planes of the hexagonal wurtzite ZnO structure, consistent with the Joint Committee on Powder Diffraction Standards (JCPDS) Card number 36-1451(A). No additional peaks were detected within the resolution limit of the diffractometer, demonstrating the production of a highly pure ZnO phase of nanoparticles [7,19].

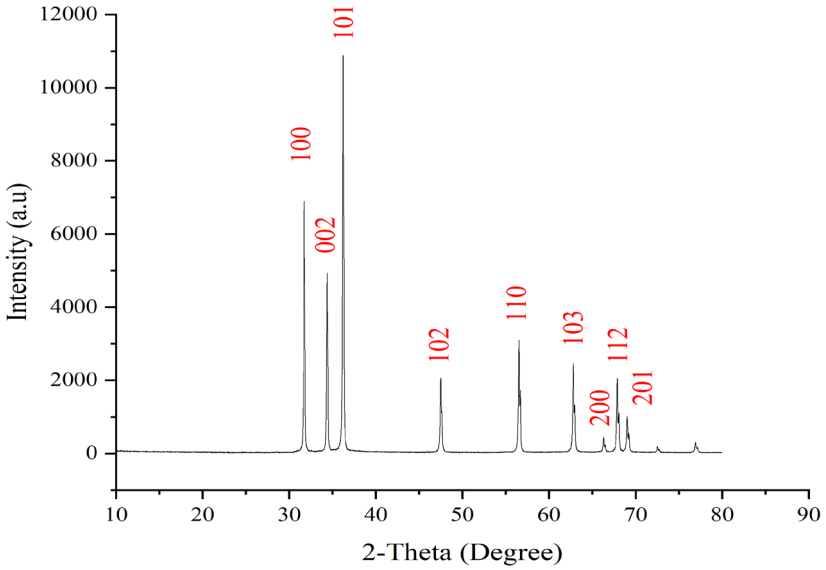

Fig. 1 *The XRD patterns of green-synthesized ZnO–PAR nanoparticles*

Deep eutectic solvents (DES) are a solvent derived from a combination of urea and choline chloride that were used as a carrier for creating nanofluids. A mixture of 1 M urea (12.01 g) and 2 M choline chloride (13.96 g) with a molar ratio of 1:2 was combined, heated in a water bath for 30 minutes at 80°C with 180 rpm, and then allowed to cool to room temperature for 10 minutes. The 0.1 wt % ZnO–PAR nanoparticles (0.1 g) were dispersed into 100 mL of DES solution using an incubator shaker at 25°C with a speed of 300 rpm for 24 hours. The ZnO–PAR solution was mixed for an entire day to increase the stability of ZnO–PAR nanofluid formation. The same procedure was carried out using 0.25 and 1wt% of ZnO–PAR nanofluids. The selection of the experimental range for the variables is in line with earlier research by Asadi et al. [20] and Qi et al. [21]. The ZnO–PAR nanofluids were stored in a closed vial at 25°C to prevent contamination until the photocatalysis testing phase. Fig. 2 demonstrates the overall synthesis of ZnO–PAR Nanofluids.

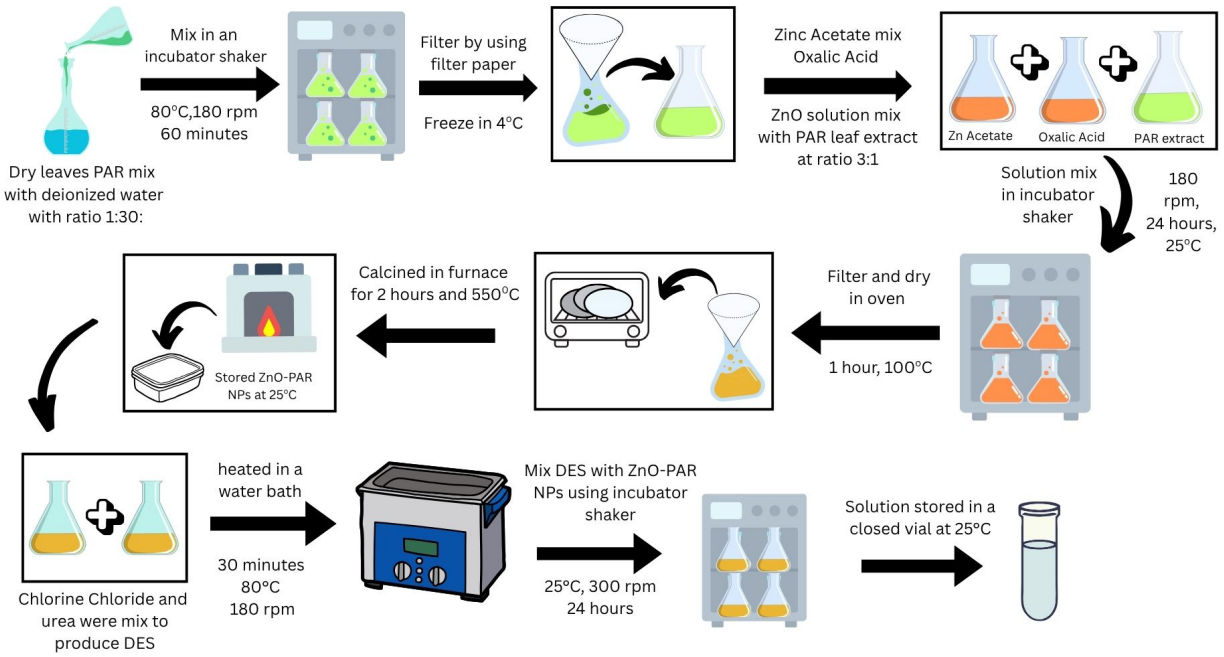

Fig. 2 *Schematic illustration of the process in producing ZnO–PAR nanofluids*

J. of Science and Technology Vol. 18 No. 1 (2026) p. 142-154

2.2 POMSE Treatment via Membrane Photocatalytic Reactors with ZnO–PAR Nanofluids

Fig. 3 depicts the MPR experimental setup employed in this investigation. The 2–L photocatalytic reactor (110 × 275 × 1.2 mm) is an essential part of the batch MPR in this study. To activate the photocatalyst, three 13 W ultraviolet (UVC light) lamps (150 mm) were placed within the reactor. Throughout the procedure, the agitator was in charge of spreading the catalyst and the molecules of the pollutants. In order to prevent membrane compaction, the membrane with an effective membrane area of 43.50 cm^2 was wetted out by circulating distilled water in the MPR under 6 bar for 30 minutes prior to the POMSE treatment experiment [6,18,19]. The ZnO–PAR nanofluids were investigated for MPR process performance with a polypiperazine–amide (PPA) nanofiltration membrane (GE Osmonics, Trisep TS40, USA).

The POMSE treatment was performed with varying ZnO types (0.1, 0.25, and 1.0 wt% ZnO–PAR nanofluids) present, with a ZnO loading of 1%, an initial POMSE concentration of 100%, and a pH of 9 solutions in the MPR. The variables' experimental range is chosen in accordance with previous study by Kamran and Qayoum [22]. To reach the adsorption–desorption equilibrium of the photocatalyst process, the POMSE and photocatalyst were thoroughly mixed for 30 minutes in the dark prior to starting the photocatalysis approach. A water chiller was used to circulate cooling water in order to maintain the operating temperature of 25 °C. After 30 minutes of photocatalysis, a Masterflex peristaltic pump was used to permeate the treated liquid through the flat sheet membrane module in crossflow filtering mode at a trans–membrane pressure of 6 bar. To avoid contamination, the treated samples were gathered and stored at 4 °C [6,7]. Each experiment will be carried out three times to guarantee repeatability. An equivalent approach was applied in MPR without ZnO for comparison.

Flux samples were collected every 5 minutes during the 180-minute experiment to evaluate the flux decline phase [18,19]. The membrane's permeability was initially determined by monitoring the flux of distilled water in an MPR device. The pure water flux and POMSE permeate flux, J ($L/m^2.h$), was calculated using equation (1)[7]

$$J = \frac{Volume\ of\ permeate\ (L)}{Area\ of\ membrane\ (m^2)\ \times\ time\ (h)} \tag{1}$$

To evaluate the behavior of membrane fouling during the reaction in MPR, the normalized flux of the membranes was computed by dividing the POMSE permeate flow by the pure water flux.

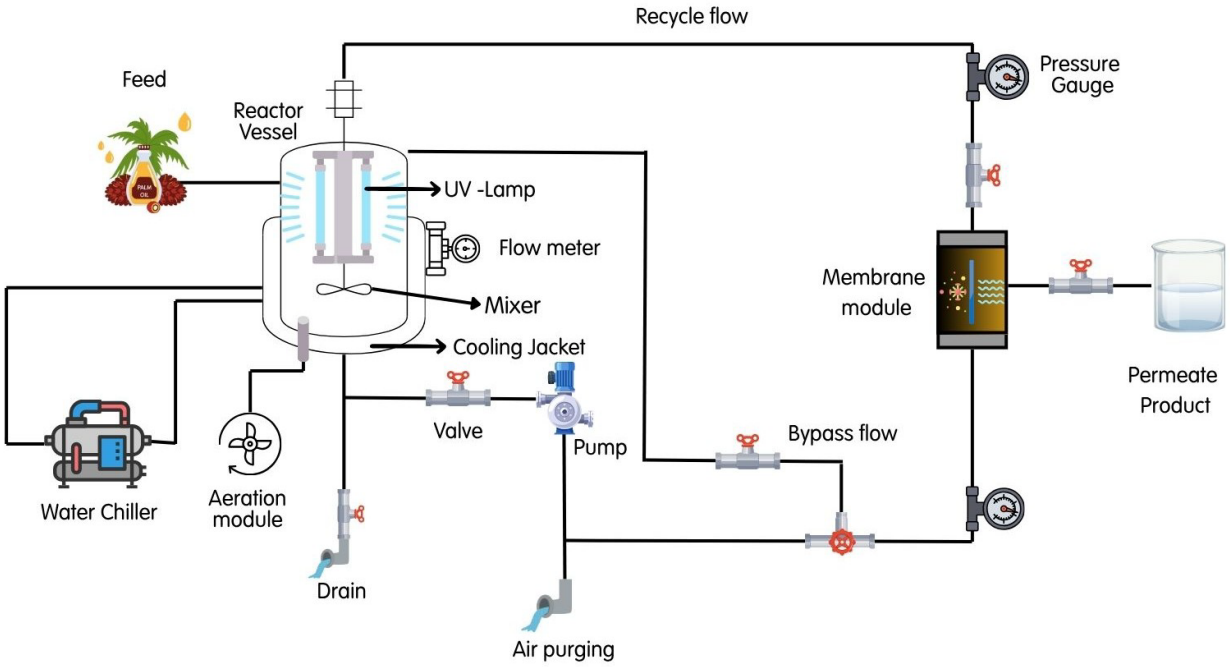

Fig. 3 *The schematic diagram of the MPR system*

2.3 Analytical Methods

The pH (benchtop pH meter Hanna HI 2550, USA), turbidity (turbidity meter HACH), total suspended solids (TSS), chemical oxygen demand (COD), and color of the untreated and treated POMSE samples were evaluated as quality criteria. Standard techniques for water and wastewater analysis were used to determine each of these water quality indicators (APHA, 2012). Standard technique 8025 was utilized to test wastewater color using a UV–Vis

spectrophotometer (Hach, DR6000TM). The standard method (Hach approach 8000) was used to do the COD analysis. The Hach digital reactor model DRB 200 (Hach, Germany) was used to heat the samples for two hours at 150°C. The sample was then cooled to room temperature for 20 minutes before being placed in the DR6000 UV–Vis spectrophotometer. The percentage of pollutants removed (RE: removal efficiency), was estimated using equation (2)[6,7].

$$\mathrm{RE}(\%) = \frac{\mathrm{Cin} - \mathrm{Cout}}{\mathrm{Cin}} \times 100 \quad (2)$$

Where C_{in} is the initial value of the POMSE quality parameter and C_{out} is the treated POMSE quality parameter at reaction time t (minute).

The shape of the membrane surface was investigated using field emission scanning electron microscopy (FESEM) (JEOL JSM–7600F). A DC sputter coater (Model: JFC1600) was used to sputter a small coating of gold over the membrane samples in order to generate electric conductivity prior to testing. Utilizing Energy Dispersion Spectrometry (EDS, JEOL–JSM 7600F, Japan), the composition of the fouling layer and membrane surface was examined.

3. Result & Discussion

3.1 Performance of MPR Incorporated ZnO–PAR NFs

Understanding the composition of POMSE contamination and determining the most effective method of treating it is essential in the treatment process. According to Table 1, POMSE wastewater has a very high level of organic content and high levels of total suspended solids (TSS), chemical oxygen demand (COD), and color. These indicators indicate the influence of organic contamination in wastewater and highlight the challenges associated with treating such effluents. Biodegradable organic matter is present in POMSE wastewater, as evidenced by the high levels of COD. A measurement of the TSS level indicates the quantity of particulate matter that can clog and foul filtering systems. Table 1 shows substantial differences in each parameter between the raw POMSE and the POMSE following MPR treatment (ZnO–PAR nanofluids 0.1wt%, 0.25wt% and1.0wt%, and without ZnO). This study found a considerable improvement in a major water quality indicator under all circumstances. The initial POMSE readings were extremely high in parameter, indicating that POMSE has a high level of contaminants. The COD, color, TSS, and turbidity levels in treated POMSE decrease as the concentration of nanofluids increases to 1.0 wt%. This might be because there are more superoxide and hydroxyl radicals, which increases the photocatalyst's surface activity. As a result, the rate of degradation rises in tandem with the nanofluids concentration. The increased nanoparticle dispersion of the ZnO–PAR nanofluids created could explain the small variation in the water quality results. As contrast to when ZnO–PAR nanofluids were present, it was evident that the quality parameter of POMSE without ZnO showed a lower value. The decrease in lignin and tannin components found in POMSE may have contributed to the breakdown of organic pollutants using the modified ZnO–PAR nanofluids, which improved the water quality performance. It has been demonstrated that MPR treatment of POMSE is successful in treating high strength wastewater due to minor variations in each parameter for each circumstance.

Table 1 *POMSE characteristics before and after MPR at various concentrations of ZnO–PAR nanofluids and without ZnO*

Parameter	Untreated POMSE	POMSE Characteristic after treatment under different types of Nanofluid concentrations			
		0.1 wt %	0.25 wt %	1.0 wt %	Without ZnO
Colour PtCO	1581.0±6.6	15.3±7.8	8.0±2.7	13.3±5.8	23.0±1.7
COD (mg/L)	460.0±62.5	10.3±0.6	21.3±4.6	36.7±5.8	58.0±1.0
Turbidity (NTU)	21.0±2.0	0.3±0.1	0.2±0.1	0.9±0.1	3.5±0.1
TSS (mg/L)	523.3±5.8	63.3±5.8	16.7±5.8	33.3±5.8	86.3±0.6

The effectiveness of POMSE removal under different ZnO–PAR nanofluids concentrations and without ZnO nanoparticles, is illustrated in Fig. 4. In comparison to the non–ZnO system, the result shows that the addition of ZnO–PAR nanofluids greatly increase removal efficiency in all parameters. ZnO–PAR nanofluids produced the maximum COD removal (99.1%) at 0.1 wt% and was highly effective in TSS (87.9%) and color removal (99.0%). The increased COD removal at lower concentrations (0.1 wt%) could be attributed to the well-dispersed nanoparticles in ZnO-PAR nanofluids, which contribute to the nanofluids' higher stability. On the other hand, the COD removal rate decreased somewhat with concentration, reaching 96.8% at 1 wt%, which could be attributed

J. of Science and Technology Vol. 18 No. 1 (2026) p. 142-154

to nanoparticle aggregation or oversaturation. TSS elimination was further optimized to 96.8% by increasing the concentration to 0.25 wt%, while color removal achieved the greatest value of 99.5%. Raising the concentration from 0.1 to 0.25 wt% will improve the removal efficiency of water quality. Malika and Sonawane [23] obtained similar results, showing that the concentration of nanofluids accelerated the degradation of dyes. Additionally, the system without ZnO had the lowest efficiency, the research suggests that ZnO–based nanofluids are essential for improving water quality. According to the study's findings, the MPR technique of treating POMSE with ZnO–PAR nanofluids (1.0 wt%) was crucial for raising the quality of treated POMSE in order to satisfy Act 127, the standard discharge requirement set forth in the Environmental Quality Act of 1974.

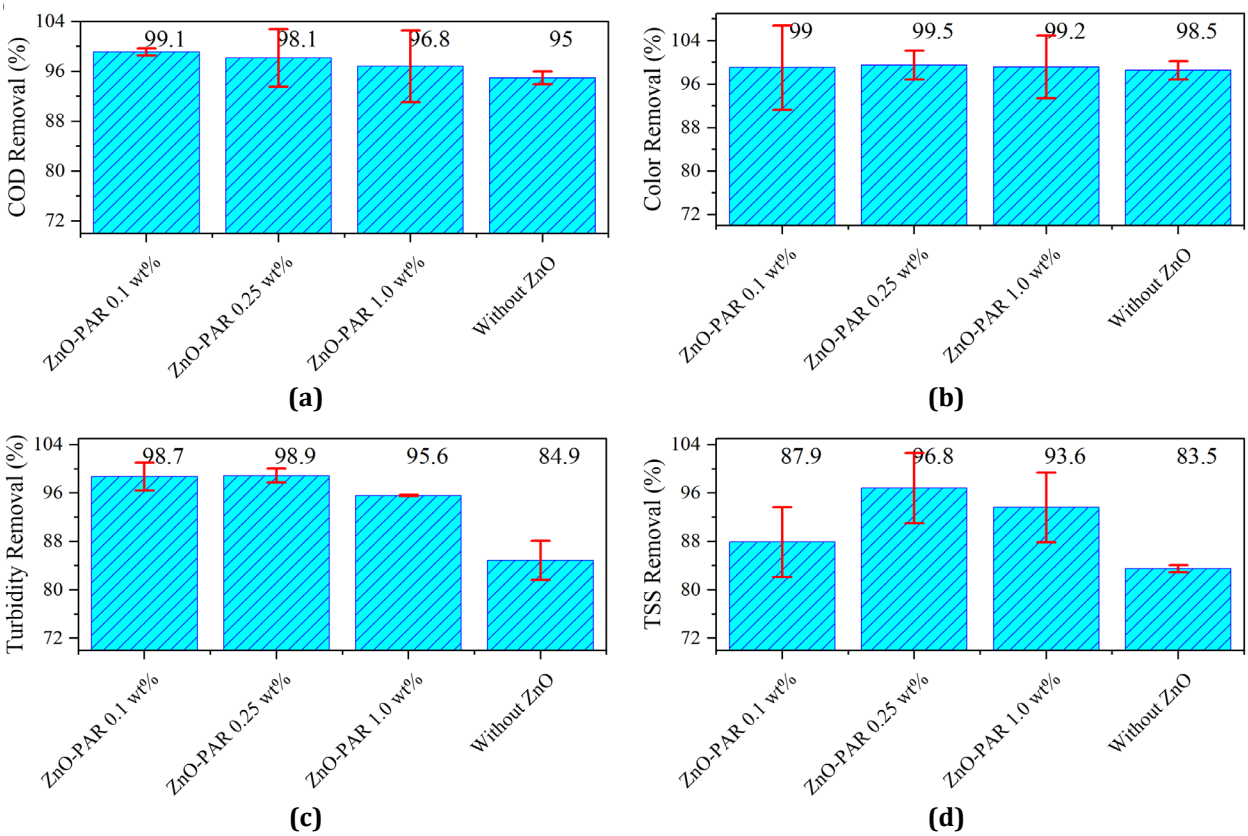

Fig. 4 *Water quality removal efficiency of treated POMSE at various ZnO–PAR nanofluids concentrations and without ZnO in terms of (a) COD; (b) Color; (c) Turbidity; and (d) TSS*

Following three hours of POMSE treatment, the change in permeate and normalized flux was used to observe the behavior of membrane fouling. Fig. 5 compares permeate and normalized flux for 0.1, 0.25 and 1.0 wt% of ZnO–PAR nanofluids, and without ZnO during POMSE nanofiltration at constant pressure. The ZnO–PAR 1.0 wt% nanofluids' green synthesis had a higher permeate flux (23.9±0.3 L/m^2.hr) and normalized flux (47 %), followed by ZnO–PAR nanofluids 0.25 wt% (22.5±1.0 L/m^2.hr, 40 %), ZnO–PAR nanofluids 0.1 wt% (21.9±1.2 L/m^2.hr, 38 %), and in the absence of ZnO (13.2±0.5 L/m^2.hr, 26%). This pattern implied that the usage of modified ZnO–PAR nanofluids with a high concentration may be responsible for the rise in the permeate flux of POMSE. The performance of nanofluids improved linearly with increasing nanofluid concentration due to increased adsorption of POMSE pollutant molecules on active sites with larger surface area due to more nanoparticles dispersed in the base liquid at higher concentration of ZnO–PAR nanofluids. Increased permeate flow and reduced membrane fouling in the MPR system were linked to improvements in the normalized flux of POMSE. When compared to ZnO–free solutions, this clearly showed that using ZnO–PAR nanofluids 1.0 wt% with a higher surface area is a major technique for enhancing and minimizing fouling in the MPR system. POMSE pretreatment enhanced flow behavior and decreased membrane fouling in the photocatalytic destruction of organic particles.

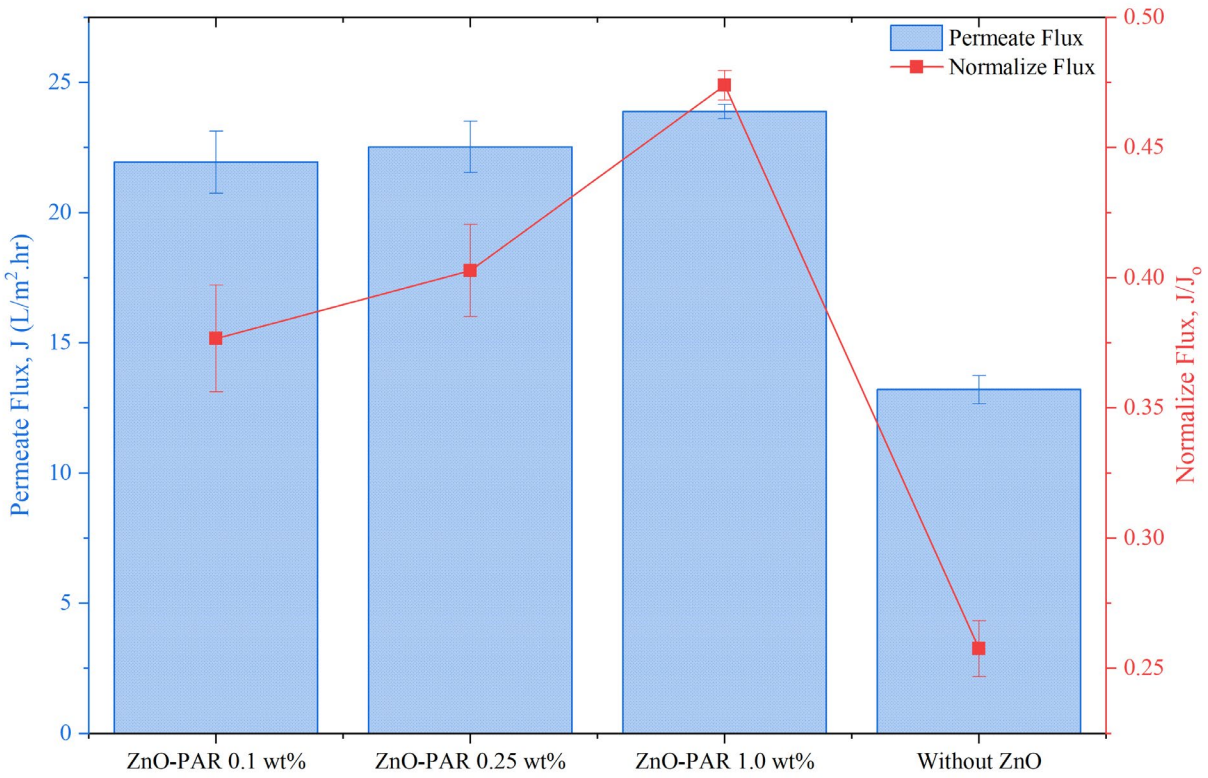

Fig 5 *Permeate and normalize flux of treated POMSE at various ZnO–PAR nanofluids concentrations and without ZnO*

The normalized flux results suggest that 1.0 wt% ZnO–PAR nanofluids have the greatest stable retention over time when compared to other concentrations (0.1 and 0.25 wt%) and without ZnO. It is noticed that the maximum concentration (1.0 wt%) is excellent for flux and fouling reduction, but the lowest concentration (0.1 wt%) is the most effective for COD removal. This higher performance is due to the appropriate nanoparticle concentration, which improves membrane antifouling capabilities while preventing pore blockage [24]. A significant decrease in flux was seen in ZnO–PAR nanofluids at lower concentrations, most likely due to membrane fouling and nanoparticle aggregation[25]. The poor performance of the 0.1 wt% ZnO–PAR nanofluids indicates that there was insufficient nanoparticle coverage to effectively prevent fouling, which is consistent with Li et al. [10]. Furthermore, it suggests that their modified surfaces or smaller particle sizes would boost dispersion stability and lower their potential for fouling [26]. Additionally, MPR without ZnO NPs had the lowest normalized flux, demonstrating the critical role of nanoparticles in preserving permeate flow and minimizing fouling [6]. These findings are consistent with previous research emphasizing the importance of adjusting nanoparticle concentration and size for wastewater treatment applications.

3.2 Membrane Characterization

FESEM displays the surface morphology of membranes used for POMSE filtering in the MPR system. A noticeable alteration in membrane structure is seen with varying ZnO–PAR nanofluid concentrations, as illustrated in Fig. 6. The roughest membrane surface, with a non–uniform particle sized ranging from 77 – 167 nm dispersion and noticeable fouling, is found at 0.1 wt% ZnO–PAR in Fig. 6(a). The presence of accumulated pollutants and irregular structures suggests significant membrane obstruction, which may have caused a slight decline in filtering effectiveness.

However, the membrane treated with 0.25 wt% ZnO–PAR shows a notably smoother and more ordered surface with particle size ranged from 54 – 243 nm, as seen in Fig. 6(b). The homogeneity and cleanliness of this membrane structure are associated with improved removal efficiency for color, turbidity, and COD, indicating that this concentration offers optimal filtering conditions by minimizing fouling and maintaining membrane permeability. Fig. 6(c), which shows the membrane exposed to 1.0 wt% ZnO–PAR, shows a more compact and homogenous surface than 0.1 wt% despite some aggregation (87 – 255 nm). The small decrease in turbidity

J. of Science and Technology Vol. 18 No. 1 (2026) p. 142-154

removal may be explained by the existence of larger particle clusters, which may partially obstruct the membrane pores while maintaining respectable COD and color removal efficacy.

The FESEM images, which demonstrate that the concentration of the nanofluid significantly affects the form of the membrane surface, typically corroborate the observed treatment results. The critical role that nanofluid concentration plays in membrane–based wastewater treatment systems is highlighted by the apparent improvement in membrane performance and cleanliness at the best concentration of 1.0 wt% ZnO–PAR. The FESEM images clearly corroborate the performance patterns and highlight the role of nanofluid concentration in improving treatment efficacy.

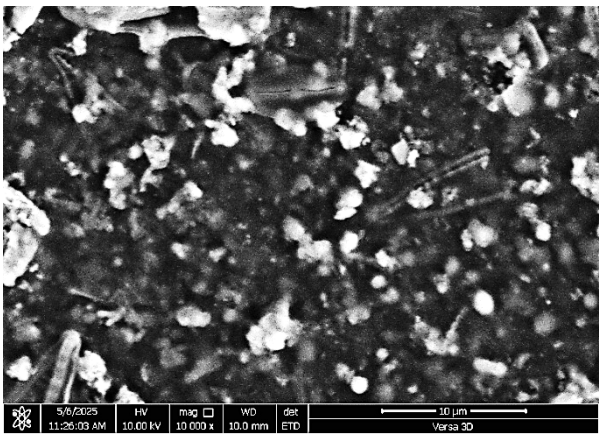

(a)

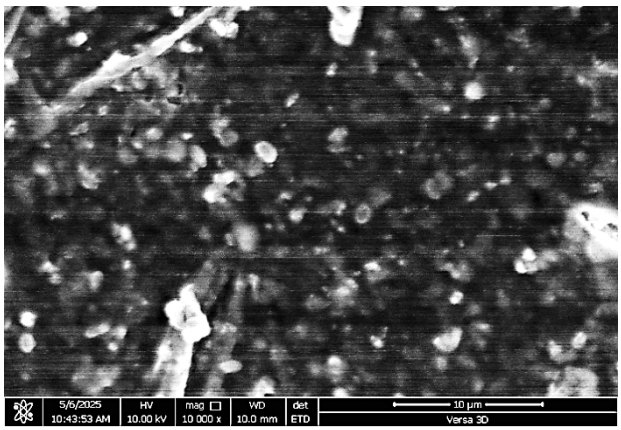

(b)

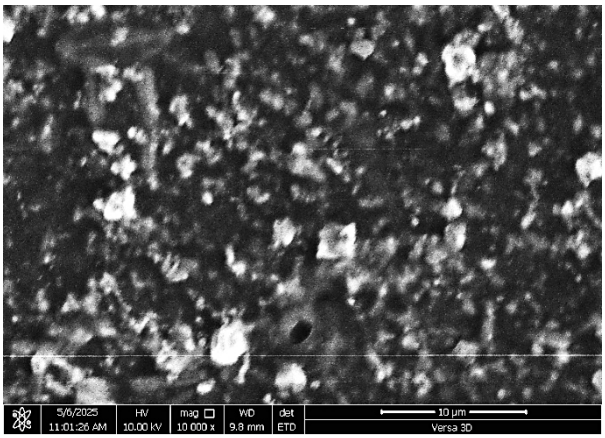

(c)

Elements	Weight (Wt %)			
	Fresh membrane	0.1 wt%	0.25 wt%	1.0 wt%
Carbon (C)	82.14	66.41	56.63	61.41
Oxygen (O)	13.53	25.76	25.67	20.93
Sulfur (S)	4.33	1.98	0.76	1.53
Chlorine (Cl)	0	1.19	1.99	0.95
Zinc (Zn)	0	4.66	14.95	15.18

(d)

Fig. 6 *FESEM image of a fouled membrane with (a) 0.1 wt%; (b) 0.25 wt%; and (c) 1.0 wt% present ZnO–PAR nanofluids; and (d) EDS analysis of the membrane surface at different concentrations of ZnO–PAR nanofluids*

The EDX evaluation clearly showed that the element of the membrane after filtering with ZnO–PAR nanofluids at different concentrations differed from the fresh membrane (Fig. 6(d)). The fact that Zinc, Oxygen and chlorine are formed on the membrane surface indicates that ZnO–PAR nanofluids are trapped there. The chlorine element on the membrane surface could be the result of residual choline chloride in the DES, which served as a carrier to synthesize ZnO-PAR nanofluids. Consequently, this suggests that the MPR method will successfully interact with and degrade contaminants. The following analysis in Fig. 6(d) shows a considerable decrease in sulfur (S) concentration and a rise in oxygen (O) concentration, as observed more clearly at 1.0 and 0.25 wt%. These alterations show that oxidative degradation or breakdown has taken place as a result of reactive oxygen species (ROS) adhering to the membranes from the UV light associated with the MPR's UV wavelength. This outcome is corroborated by the decrease in deposits on the membrane surface (Fig. 6a–c), where a thin layer of foulant developed following filtering with concentrations of 1.0 and 0.25 wt% of ZnO–PAR nanofluids. This effect is most likely caused by the breakdown of certain contaminants in POMSE during the photocatalytic reaction, which then increases the permeate flux at greater nanofluid concentrations. Therefore, in subsequent research, the concentration of ZnO–PAR nanofluids must be appropriately optimized for photocatalytic performance and stability.

3.3 The Performance of Photocatalytic and MPR Incorporated ZnO–PAR Nanofluids

Fig. 7 shows the removal efficiency of water quality parameters utilizing photocatalytic and MPR systems at varying concentrations of ZnO–PAR nanofluids. The MPR system was demonstrated to be more efficient than photocatalytic technology in treating POMSE in terms of turbidity, TSS, and COD removal, with maximum percentages ranging from 96 to 99%. Conversely, the removal performance of the photocatalytic process ranges from 62% to 84%. The most notable difference in color removal efficacy between MPR (99%) and photocatalytic alone (12-32%), could be attributed to POMSE's capacity to degrade pollutants, comprising complex lignin and tannin molecules. Higher lignin and tannin concentrations in POMSE make it difficult to break down and have a significant impact on its color [27]. In the MPR approach, it appears that the tiny nanofiltration membrane pores used in this study may prevent large molecules from entering the membrane pores, hence improving water quality after filtration. As demonstrated in Fig. 7, photocatalytic adsorption has been shown to function as a pretreatment for POMSE prior to membrane filtration, reducing membrane fouling and improving the efficacy of water quality removal. This clarifies that the combined treatment, which incorporates membrane and photocatalytic processes, provides numerous advantages. The photocatalytic process breaks down pollutant particles, resulting in smaller POMSE particles and higher quality penetrates.

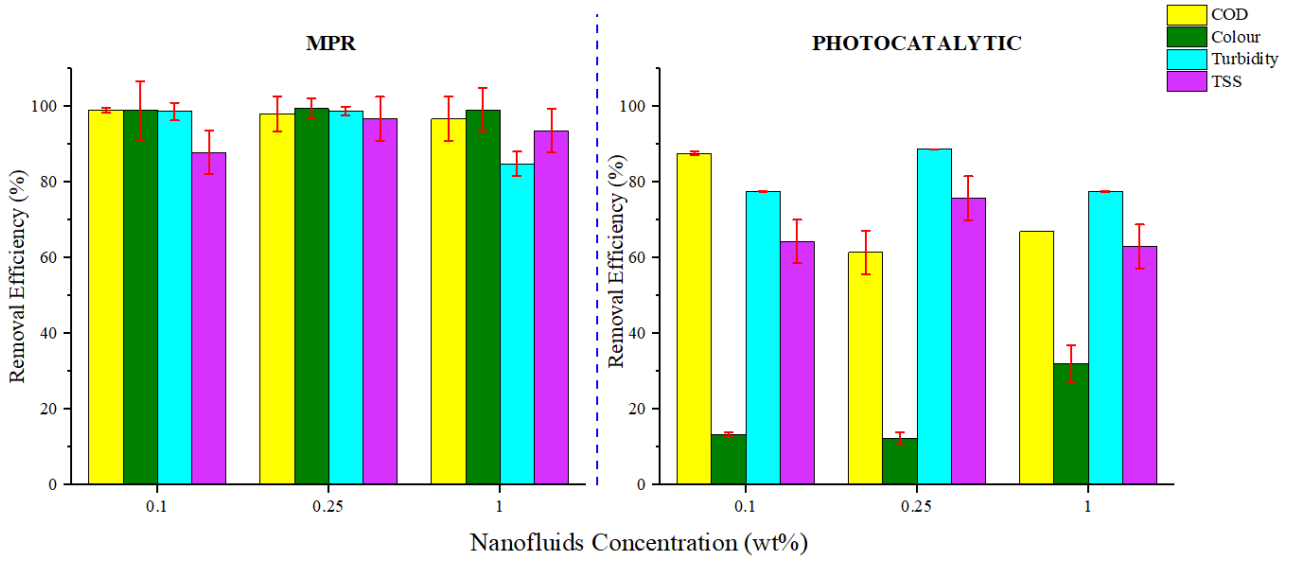

Fig 7 *Photocatalytic and MPR performance on water quality efficiency of POMSE treatment*

The performance improvement trend of both approaches is quite similar at varying nanofluid concentration. As the concentration of ZnO–PAR nanofluids increase, more photocatalyst zones become available for UV light absorption and POMSE pollutant elimination. Similar trends of increased removal effectiveness utilizing the MPR approach combined with nanoparticles were also demonstrated in the earlier work by Kusworo et al. [28] and Sidik et al. [7]. The results of this study demonstrated that the use of ZnO–PAR nanofluids enhanced the dispersion of liquid form photocatalyst in the POMSE in comparison to solid form nanoparticles from previous study Sidik et al. [7]. Consequently, the interaction between the photocatalyst and POMSE pollutants may enhance and boost the efficacy of the MPR treatment process.

The improved adsorption capability of ZnO–PAR nanofluids is due to their unique structural characteristics. Higher ZnO–PAR nanofluid stability throughout the synthesis process is provided by the shape of ZnO nanoparticles capping with extracted PAR leaves. This process is thought to enhance adsorption and photocatalytic destruction of POMSE pollutants. The ZnO–PAR nanofluids are believed able to breaks down organic pollutants in POMSE into CO_2 and H_2O, which reduces membrane fouling. Photocatalytic adsorption reduces pollutant deposition on the membrane surface by lowering the organic pollutant in POMSE molecules before nanofiltration. This prolongs operational efficiency with a higher average flux of up to 45%. Thus, the results of this investigation demonstrate that ZnO–PAR nanofluids that can reduce the fouling rate improve membrane permeability and selectivity while lowering the frequency of cleaning and prolonging membrane life.

4. Conclusion

This study demonstrated that employing ZnO–PAR nanofluids at 0.1, 0.25, and 1.0 wt% to treat POMSE in an MPR system resulted in the best balanced and efficient performance in terms of COD, color, turbidity, and TSS removal,

with efficiencies ranging from 93% to 99%. FESEM and EDS tests confirmed that ZnO–PAR 1.0 wt% likewise showed a higher normalized flux (47%) and decreased membrane fouling. Pollutant agglomeration effects may result in a minor decrease in flux stability at 0.1 and 0.25 wt% ZnO–PAR nanofluids concentrations. This behavior is explained by the fact that a lower concentration of ZnO–PAR nanoparticles in the base liquid nanofluid reduces photocatalytic degradation and, as a result, increases membrane fouling. Meanwhile, lesser concentrations of 0.1 wt% result in increased COD removal due to the well-dispersed nanoparticles in nanofluids. The findings demonstrate that increasing photocatalytic activity, membrane performance, and overall treatment efficiency all depend on controlling nanofluid concentration. As a result, using ZnO–PAR nanofluids in MPR systems at the right concentration has a lot of promise as a tertiary treatment strategy to satisfy strict POMSE discharge requirements. Furthermore, continued research and development to maximize the commercial viability of ZnO–PAR nanofluids in MPR systems is recommended in the future.

Acknowledgement

This research was supported by the Ministry of Higher Education (MOHE) through the Fundamental Research Grant Scheme (FRGS/1/2023/TK08/UTHM/02/3) (K477) and by Universiti Tun Hussein Onn Malaysia through Tier 1 funding (Vot Q439).

Conflict of Interest

Authors declare that there is no conflict of interest regarding the publication of the paper.

Author Contribution

The authors confirm contribution to the paper as follows: ***study conception and design:*** *Dilaeleyana Abu Bakar Sidik, Nur Hanis Hayati Hairom;* ***data collection:*** *Muhammad Akmal Annuar, Muhammad Zharif Mohd Zamirullah, Noor Atiqah Zuraini;* ***analysis and interpretation of results:*** *Zarizi Awang, Maskhairiah Ismail;* ***draft manuscript preparation:*** *Muhammad Akmal Hisyam Idris. All authors reviewed the results and approved the final version of the manuscript.*

References

[1] Nawaz, R., Kait, C. F., Chia, H. Y., Isa, M. H., Huei, L. W., Sahrin, N. T., & Khan, N. (2021) Countering major challenges confronting photocatalytic technology for the remediation of treated palm oil mill effluent: A review. *Environmental Technology and Innovation,23,* 101764, https://doi.org/10.1016/j.eti.2021.101764

[2] Saputera, W. H., Amri, A. F., Daiyan, R., & Sasongko, D. (2021) Photocatalytic technology for palm oil mill effluent (POME) wastewater treatment: Current progress and future perspective. *Materials*, *14(11),* 2846, https://doi.org/10.3390/ma14112846

[3] Ahmed, Y., Maya, A. A. S., Akhtar, P., AlMohamadi, H., Mohammad, A. W., Ashekuzzaman, S. M., Olbert, A. I., & Uddin, M. G. (2025) Advancements and challenges in Fenton-based advanced oxidation processes for antibiotic removal in wastewater: From the laboratory to practical applications, *Journal of Environmental Chemical Engineering, 13(1)*, 115068, https://doi.org/10.1016/j.jece.2024.115068

[4] Hu, W., Yang, D., Chang, Y., Yu, K., Yang, L., Yan, W., Xu, H., & Wu, X. (2024) Electrocatalytic oxidation for organic wastewater: Recent progress in anode material, reactor, and process combination, *Chemical Engineering Journal, 496,* 154120, https://doi.org/10.1016/j.cej.2024.154120

[5] Molinari, R., Argurio, P., Szymański, K., Darowna, D., & Mozia, S. (2020) Photocatalytic membrane reactors for wastewater treatment. *Current Trends and Future Developments on (Bio-) Membranes*. 83-116, https://doi.org/10.1016/B978-0-12-816823-3.00004-6

[6] Awang, Z., Hayati Hairom, N. H., Abdul Hamid, N. H., Bakar Sidik, D. A., Hasanah Mohd Nadzim, U. K., Madon, R. H., & Yong, N. L. (2024). Palm oil mill secondary effluent treatment using ZNO-clay liquid photocatalyst in membrane photocatalytic reactor. *Journal of the Indian Chemical Society, 101(7),* 101158. https://doi.org/10.1016/J.JICS.2024.101158

[7] Sidik, D. A. B., Hairom, N. H. H., Ahmad, M. K., Madon, R. H., & Mohammad, A. W. (2020) Performance of membrane photocatalytic reactor incorporated with ZnO-Cymbopogon citratus in treating palm oil mill secondary effluent. *Process Safety and Environmental Protection, 143,* 273-284, https://doi.org/10.1016/j.psep.2020.06.038

[8] Koe, W. S., Lee, J. W., Chong, W. C., Pang, Y. L., & Sim, L. C. (2020) An overview of photocatalytic degradation: photocatalysts, mechanisms, and development of photocatalytic membrane. *Environmental Science and Pollution Research, 27(3),* 2522-2565, https://doi.org/10.1007/s11356-019-07193-5

[9] Zainuri, N. Z., Hairom, N. H. H., Sidik, D. A. B., Desa, A. L., Misdan, N., Yusof, N., & Mohammad, A. W. (2018) Palm oil mill secondary effluent (POMSE) treatment via photocatalysis process in presence of ZnO-PEG nanoparticles. *Journal of Water Process Engineering, 26,* 10-16, https://doi.org/10.1016/j.jwpe.2018.08.009

[10] Li, X., Chen, Y., Tao, Y., Shen, L., Xu, Z., Bian, Z., & Li, H. (2022). Challenges of photocatalysis and their coping strategies. *Chem Catalysis 2(6)*, 1315-1345, https://doi.org/10.1016/j.checat.2022.04.007

[11] Pauzi, N., Zain, N. M., & Yusof, N. A. A. (2020) Gum arabic as natural stabilizing agent in green synthesis of ZnO nanofluids for a ntibacterial application, Journal of Environmental Chemical Engineering, 8(3), 103331, https://doi.org/10.1016/j.jece.2019.103331

[12] Yahya, N. Y., Chan, J. X., & Ngadi, N. (2021) Biosorption of chromium (Vi) ions using sustainable eggshell impregnated pandanus amaryllifolius roxb. Biosorbent. *Evergreen, 8(1),* 146-155, https://doi.org/10.5109/4372271

[13] Haththotuwa, S.L.G., & Amarasinghe, B.M.W.P.K. (2023) Batch Adsorption Study for the Removal of Textile Dyes from Aqueous Solutions Using Pandanus Amaryllifolius (Rampe) Leaves. *ICSBE 2022. Lecture Notes in Civil Engineering, 362,* 75-87, https://doi.org/10.1007/978-981-99-3471-3_6

[14] Wang, W., Ren, Z., Zheng, S., Wu, H., Li, P., Peng, W., Su, W., & Wang, Y. (2024) Botany, phytochemistry, pharmacology, and applications of Pandanus amaryllifolius Roxb.: A review. *Fitoterapia, 177*, 106144, http://doi: 10.1016/J.FITOTE.2024.106144

[15] Drummer, S., Madzimbamuto, T., & Chowdhury, M. (2021) Green synthesis of transition-metal nanoparticles and their oxides: A review. *Materials 14(11)*, 2700, https://doi.org/10.3390/ma14112700

[16] Adhamatika, A ., Murtini E. S., & Sunarharum W. B. (2021) The effect of leaf age and drying method on physico-chemical characteristics of pandan (Pandanus amaryllifolius Roxb.) leaves powder. *International Conference on Green Agro-industry and Bioeconomy*, 733, 012073. doi:10.1088/1755-1315/733/1/012073

[17] Zuraini, N.A., Sidik, D.A.B., Shamhan, S.D., Harom, N.H.H., Suradi, S.S., Madon, R.H., Awang, Z., Hamid, N.H.A., Adnan, R.M., & Halim, N.A. (2025) Photocatalytic reactor incorporating modified zinc oxide Acorus calamus nanoparticles to remediate palm oil mill effluent. *Malaysian Journal of Analytical Sciences*, 29(2) 1290.

[18] Sidik, D.A.B., Hairom, N.H.H., & Mohammad, A.W. (2019) Performance of membrane types in PMR for POMSE. *Process Safety and Environmental Protection*, 130, 265–274. https://doi.org/10.1016/j.psep.2019.08.018.

[19] Sidik, D.A.B., Hairom, N.H.H., Mohammad, A.W., Halim, N.A., Ahmad, M.K., & Hamzah S. (2020) Fouling control strategies in membrane photocatalytic reactors. *Chemical Engineering Research and Design*, 162, 12–27. https://doi.org/10.1016/j.cherd.2020.07.021.

[20] Asadi, A., Aberoumand, S., Moradikazerouni, A., Pourfattah, F., Żyła, G., Estellé, P., Mahian, O., Wongwises, S., Nguyen, H. M., & Arabkoohsar, A. (2019) Recent advances in preparation methods and thermophysical properties of oil-based nanofluids: A state-of-the-art review. *Powder Technology, 352,* 209-226. https://doi.org/10.1016/j.powtec.2019.04.054

[21] Qi, C., Luo, T., Liu, M., Fan, F., & Yan, Y. (2019) Experimental study on the flow and heat transfer characteristics of nanofluids in double-tube heat exchangers based on thermal efficiency assessment. *Energy Conversion and* Management, 197, 111877, https://doi.org/10.1016/j.enconman.2019.111877

[22] Kamran, M., & Qayoum, A. (2022) Effect of ZnO nanofluids on thermo-hydraulic characteristic of flow in a heated duct. *Energy Sources, Part A: Recovery, Utilization, and Environmental Effects*, 44(4), 10681–10693. https://doi.org/10.1080/15567036.2022.2154871

[23] Malika, M., & Sonawane, S. S. (2022) The sono-photocatalytic performance of a Fe2O3 coated TiO2 based hybrid nanofluid under visible light via RSM. *Colloids and Surfaces A: Physicochemical and Engineering Aspects, 641,* 128545, https://doi.org/10.1016/j.colsurfa.2022.128545

[24] Ayyaru, S., Dinh, T. T. L., & Ahn, Y. H. (2020) Enhanced antifouling performance of PVDF ultrafiltration membrane by blending zinc oxide with support of graphene oxide nanoparticle. *Chemosphere, 241*, 125068, https://doi.org/10.1016/j.chemosphere.2019.125068

[25] Purushothaman, M., Harikrishnan, A., Senthil Kumar, P., George, J., Rangasamy, G., & Vaidyanathan, V. K. (2023) Enhancement of antifouling properties, metal ions and protein separation of poly(ether-ether-sulfone) ultrafiltration membranes by incorporation of polyethylene glycol and n-ZnO. *Environmental Research, 216,* 114696, https://doi.org/10.1016/j.envres.2022.114696

[26] Yang, X., Ma, X., Yuan, J., Feng, X., Zhao, Y., & Chen, L. (2023). Enhanced the antifouling and antibacterial performance of PVC/ZnO-CMC nanoparticles ultrafiltration membrane. *Journal of Applied Polymer Science, 140(5),* e53412, https://doi.org/10.1002/app.53412

[27] Ujang, F. A., Roslan, A. M., Osman, N. A., Norman, A., Idris, J., Farid, M. A. A., Halmi, M. I. E., Gozan, M., & Hassan, M. A. (2021) Removal behaviour of residual pollutants from biologically treated palm oil mill effluent by Pennisetum purpureum in constructed wetland. *Scientific reports,* 11, 18257. https://doi.org/10.1038/s41598-021-97789-0

[28] Kusworo, T. D., Kumoro, A. C., Puspaningrum, F., Ramadhani, M. N., Puspa, M. B., Utomo, D. P., & Kurniawan, T. A. (2025) Integration of photocatalytic-adsorption pre-treatment with ternary nanocomposite-based PVDF-Bi_2WO_6/CeO_2/MoS_2 photocatalytic membrane for enhanced treatment of natural rubber processing wastewater. Journal of Environmental Chemical Engineering, 13(4), 117253. https://doi.org/10.1016/J.JECE.2025.117253